PHILIPS

www.philips.com

Image Quality Assessment and Perceptual Optimization

No-reference IQA via Non-local Modeling

Shuyue Jia

M.Phil. Student

April 2023

innovation + you

Learning Objectives

- **What is** Objective Image Quality Assessment (IQA)?
- **Why do we need** IQA with Perceptual Optimization?
- Current **Related Work**
- A **Proposed Non-local Modeling method** for IQA

Note: Subjective IQA: Image quality collected from human subjects (observers)

What is Image Quality Assessment (IQA)? Synthetic Distortion

Reference/Pristine Image

Distorted Image
by Gaussian Noise

Image Credit: Shuyue Jia and Ka-Po Chan

What is Image Quality Assessment (IQA)? Authentic Distortion

Reference/Pristine Image

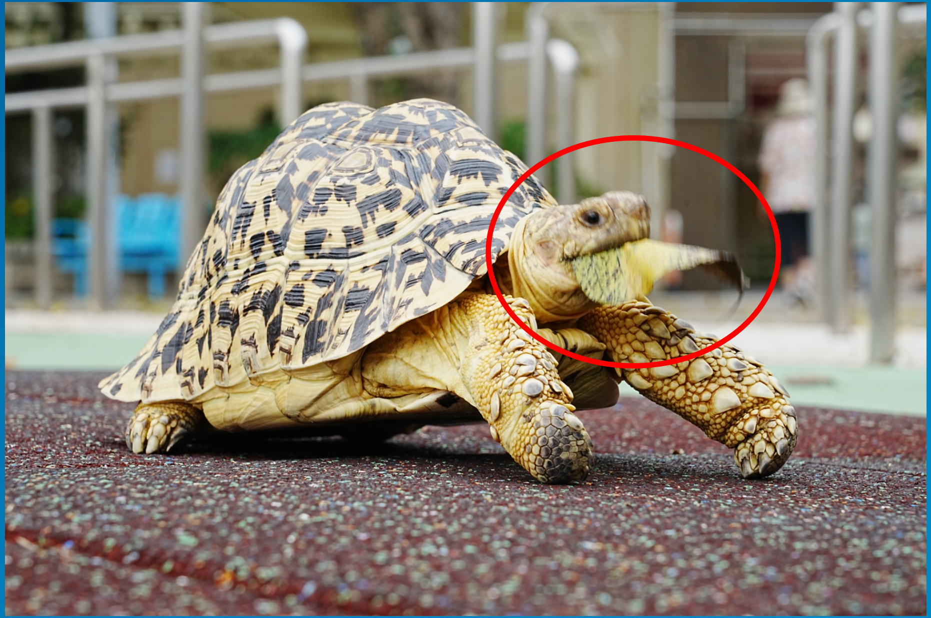

Motion Blur
due to low shutter speed

Image Credit: Shuyue Jia and Ka-Po Chan

Problem Definition

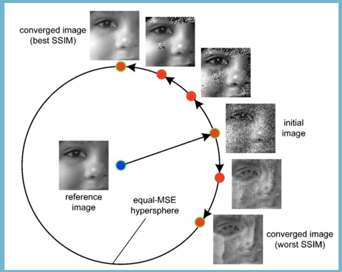

Definitions

- *Natural Image*: images captured by optical cameras
- *Fidelity:* keep the content of the distorted images (semantic information) unchanged
- *Image Quality (Fidelity) Assessment:* measure the input image's visual (perceptual) quality
- *Visual Quality and Perceptual Optimization*: people's overall subjective visual experience when viewing images
- *Synthetic Distortion:* synthetic distortions added to the whole area of image (mainly global uniform distortions)
- *Authentic Distortion:* images captured in the wild include varies contents and diverse types of distortions (global uniform distortions + non-uniform distortions in local areas)

Image Quality Assessment Category

- *Full-Reference IQA*: with Reference/Pristine Image
- *Reduced-Reference IQA*: with partial information from Reference Image, *e.g.*, a subset of features
- *No-Reference (Blind) IQA: without any information from* Reference Image

Measurements

- *Label:* Mean Opinion Score (MOS) *vs. Model Output:* one scalar score
- *Pearson Linear Correlation Coefficient (PLCC):* prediction accuracy
- *Spearman Rank-order Correlation Coefficient (SRCC):* prediction monotonicity

Image Credit: Prof. Zhou Wang

Why do we need Image Quality Assessment?

"If you can't measure it, you can't improve it." (Peter Drucker)

Reference/Pristine Image

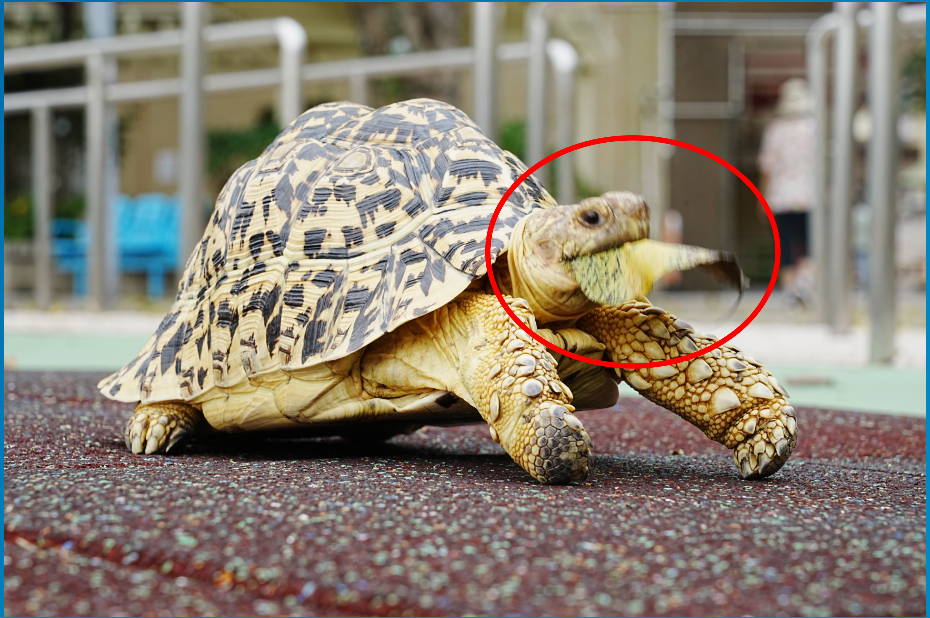

Motion Blur
due to low shutter speed

Image Credit: Shuyue Jia and Ka-Po Chan

Why do we need Image Quality Assessment?

Automatic Image Quality Assessment

Reference Image

Distorted Image

IQA Model

Image Quality

Image Credit: TID2013 Database

Why do we need Image Quality Assessment?

Performance Evaluation of Image Processing Systems

by a Full-Reference IQA Method

Distorted Image

Model Input

Image Restoration System

De-blurred Image

Model Output

Evaluation

MSE
PSNR
SSIM
LPIPS
etc.

Reference Image

Label

FR-IQA Method

Image Credit: TID2013 Database

Tools | Predictive Coding Based Multiscale Network with EncoderDecoder LSTM for Video Prediction

130% | Annotate | Edit | Scan & OCR | Export

The picture can't be displayed.

Conv-TT-LSTM 

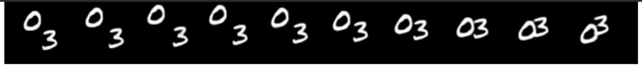

Fig. 6. Visualization examples on the KTH datasets. We use 10 frames as input to predict next 30 frames. The other results are obtained from [49]. Zoom in for a better view.

Fig. 7. Visualization examples on the MNIST datasets. We use 10 frames as input to predict next 10 frames. In each group, the first row indicates the ground truth frames and the second row indicates predicted frames. Zoom in for a better view.

B. *Experimental results*

KTH The KTH is one of the most commonly used datasets for task of video prediction. It is very popular due to its moderate complexity of scene and event (the dataset contains only 6 action categories on a simple backgrounds). Similar to previous works, we use person 1-16 for training and person 17-25 for testing, and use 10 frames as input to predict the next 30 frames. The quantitative evaluation results are shown in Table II. The results of previous works are excerpted from [25], [48] and [49]. As shown in the table, our method achieve comparable or better performance compared with the state-of-the-art methods. In addition, our model converges fast, which only takes about 30 epochs to achieve good performance. Figure 6 shows the visualization examples, our method can also achieve good visual results, while the Conv-TT-LSTM [50], which obtains the highest SSIM score, shows poor performance on the qualitative evaluation. The mismatch between quantitative and qualitative assessments remains an unsolved problem for video prediction tasks.

Moving MNIST The Moving MNIST is an early popular synthetic dataset for video representation learning. Its scenarios and events are very simple, each sequence is 20 in length and shows how 2 digits move at a constant speed and bounce within a 64×64 box. Similarly, we use 10 frames as input to predict the next 10 frames. Table III shows the quantitative evaluation results on SSIM and MSE, the results of previous works are excerpted from [57] and [48]. Figure 7 shows the visualization examples, we have tried our best to search the demonstrated examples of previous works, but unfortunately none have been found, so we only present our results in the figure. Since the scenes and events are simple, we did not use adversarial training to sharpen the generated images to save training overhead. Nevertheless, we can still achieve good performance from the perspective of qualitative evaluation. Actually, most of the background pixels in this dataset are zeros. If we set a threshold and change the predicted pixels smaller than the threshold to zeros, we will get higher accuracy

Credit: Ling *et al.*, Predictive Coding Based Multiscale Network with Encoder-Decoder LSTM for Video Prediction, Under Review

Why do we need Image Quality Assessment?

Optimizing Image Processing Systems (Model Parameter Optimization)

by a Full-Reference IQA Method

Distorted Image

Model Input

Image Restoration System

De-blurred Image

Model Output

Loss

Reference Image

Label

FR-IQA Method

Image Credit: TID2013 Database

Current Related Work of Full-Reference IQA

- **Signal Fidelity Approaches**

  Mean Squared Error (MSE) and Peak Signal-to-Noise Ratio (PSNR)

  I_p: number of pixels in the image; x_i and y_i are the i^{th} pixels of the ref. and dis.

$$\text{MSE} = \frac{1}{I_p}\sum_{i=1}^{I_p}(x_i - y_i)^2 , \qquad \text{PSNR} = 10\times \log_{10}\left(\frac{255^2}{\text{MSE}}\right).$$

- **Bottom-Up Approaches (Error Sensitivity Framework)**

  separately model each basic module of Human Visual System (HVS)

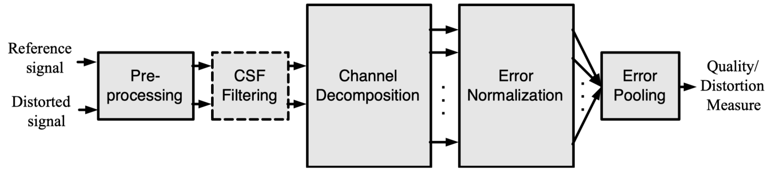

Fig. 1. A prototypical quality assessment system based on error sensitivity. Note that the CSF feature can be implemented either as a separate stage (as shown) or within "Error Normalization."

Image Credit:
SSIM Paper
(Prof. Zhou Wang)

Current Related Work of Full-Reference IQA

- Top-Down Approaches

  directly imitate the function of HVS as a single model

  Representative Work:

  (1) Structural Similarity (**SSIM**)

  (2) Visual Information Fidelity (**VIF**)

  (3) Learned Perceptual Image Patch Similarity (**LPIPS**)

Current Related Work of Full-Reference IQA

- Top-Down Approaches - Structural Similarity (SSIM)

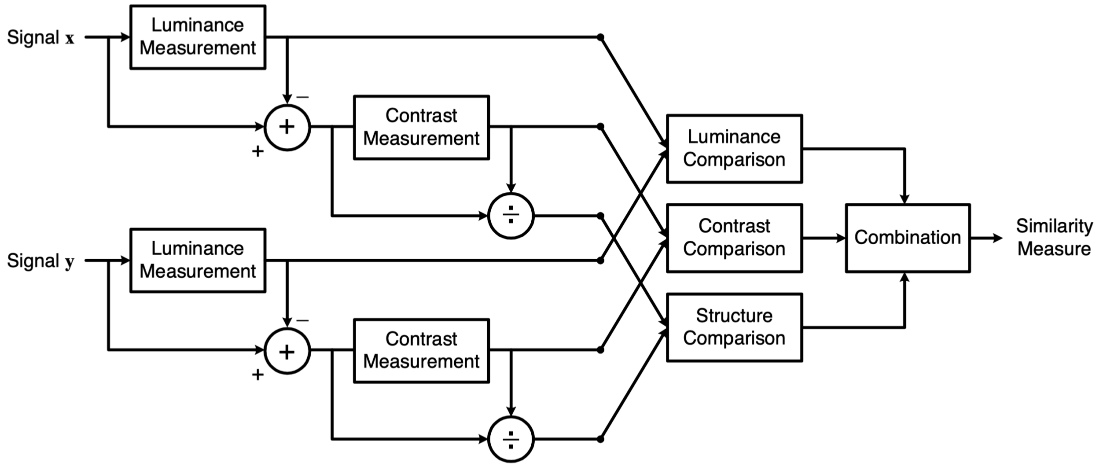

Fig. 3. Diagram of the structural similarity (SSIM) measurement system.

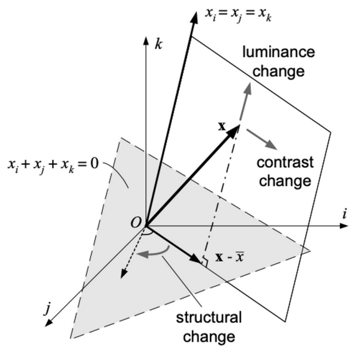

FIGURE 5 Separation of luminance, contrast and structural changes from a reference image **x** in the image space. This is an illustration in three-dimensional space. In practice, the number of dimensions is equal to the number of image pixels.

$$\mathrm{SSIM}(\mathbf{x},\mathbf{y}) = \frac{(2\mu_x\mu_y + C_1)(2\sigma_{xy} + C_2)}{(\mu_x^2 + \mu_y^2 + C_1)(\sigma_x^2 + \sigma_y^2 + C_2)}$$

μ: Mean Intensity → luminance

σ: Standard Deviation → contrast

$(\mathbf{x} - \mu_x)/\sigma_x$: normalization

Correlation of Normalized Signals → structure

Credit: Wang *et al.*, Image Quality Assessment: From Error Visibility to Structural Similarity, In IEEE T-IP'04

Current Related Work of Full-Reference IQA

- Top-Down Approaches - Visual Information Fidelity (VIF)

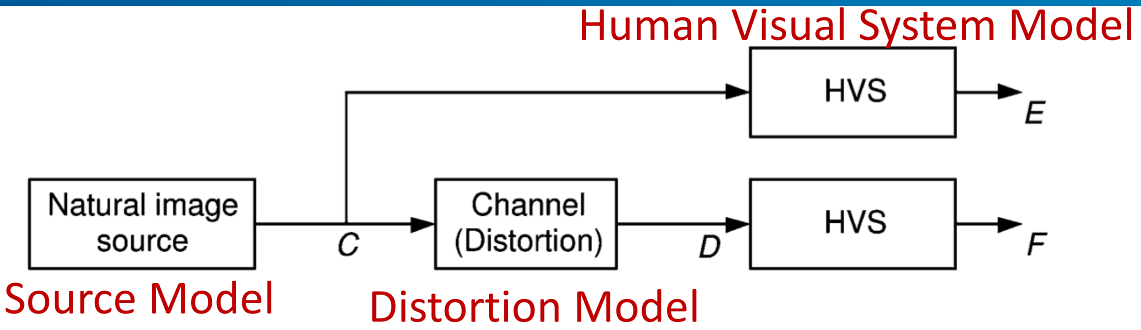

Fig. 1. Mutual information between $\mathcal{C}$ and $\mathcal{E}$ quantifies the information that the brain could ideally extract from the reference image, whereas the mutual information between $\mathcal{C}$ and $\mathcal{F}$ quantifies the corresponding information that could be extracted from the test image.

Credit: Sheikh *et al.*, Image Information and Visual Quality, In IEEE T-IP'06 and Netflix VMAF System (Prof. Jay Kuo, USC)

Current Related Work of Full-Reference IQA

- **Top-Down Approaches** - Learned Perceptual Image Patch Similarity (**LPIPS**)

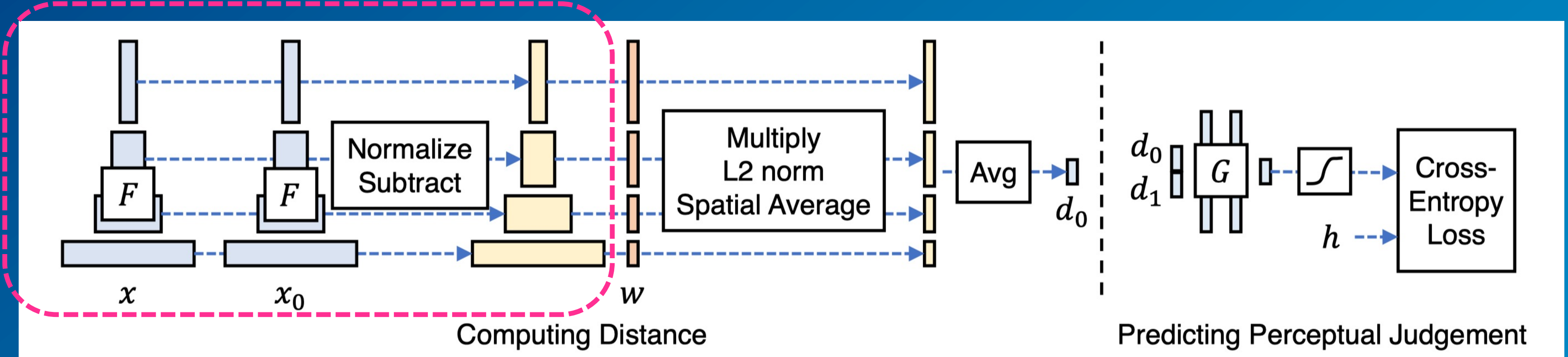

Figure 3: **Computing distance from a network** (Left) To compute a distance d_0 between two patches, x, x_0, given a network $\mathcal{F}$, we first compute deep embeddings, normalize the activations in the channel dimension, scale each channel by vector w, and take the ℓ_2 distance. We then average across spatial dimension and across all layers. (Right) A small network $\mathcal{G}$ is trained to predict perceptual judgment h from distance pair (d_0, d_1).

Based on Deep Features instead of Statistics

Credit: Zhang *et al.*, The Unreasonable Effectiveness of Deep Features as a Perceptual Metric, In CVPR'18

The picture can't be displayed.

[Paper Link]

Tools [DISTS] Image Quality Assessment- Unifying Structure and Texture Similarity

130% Annotate Edit Scan & OCR Export

This article has been accepted for publication in a future issue of this journal, but has not been fully edited. Content may change prior to final publication. Citation information: DOI 10.1109/TPAMI.2020.3045810, IEEE Transactions on Pattern Analysis and Machine Intelligence

Image Quality Assessment: Unifying Structure and Texture Similarity

Keyan Ding, Kede Ma, *Member, IEEE,* Shiqi Wang, *Member, IEEE,* and Eero P. Simoncelli, *Fellow, IEEE*

Abstract—Objective measures of image quality generally operate by making local comparisons of pixels of a “degrade” image to those of the original. Relative to human observers, these measures are overly sensitive to resampling of texture regions (*e.g.*, replacing one patch of grass with another). Here we develop the first full-reference image quality model with explicit tolerance to texture resampling. Using a convolutional neural network, we construct an injective and differentiable function that transforms images to multi-scale overcomplete representations. We empirically show that the spatial averages of the feature maps in this representation capture texture appearance, in that they provide a set of sufficient statistical constraints to synthesize a wide variety of texture patterns. We then describe an image quality method that combines correlation of these spatial averages (“texture similarity”) with correlation of the feature maps (“structure similarity”). The parameters of the proposed measure are jointly optimized to match human ratings of image quality, while minimizing the reported distances between subimages cropped from the same texture images. Experiments show that the optimized method explains human perceptual scores, both on conventional image quality databases, as well as on texture databases. The measure also offers competitive performance on related tasks such as texture classification and retrieval. Finally, we show that our method is relatively insensitive to geometric transformations (*e.g.*, translation and dilation), without use of any specialized training or data augmentation. Code is available at https://github.com/dingkeyan93/DISTS.

Index Terms—Image quality assessment, structure similarity, texture similarity, perceptual optimization.

Extension: Ding *et al.*, Comparison of Full-Reference Image Quality Models for Optimization of Image Processing Systems, In IJCV’21

Framework of Reduced-Reference IQA

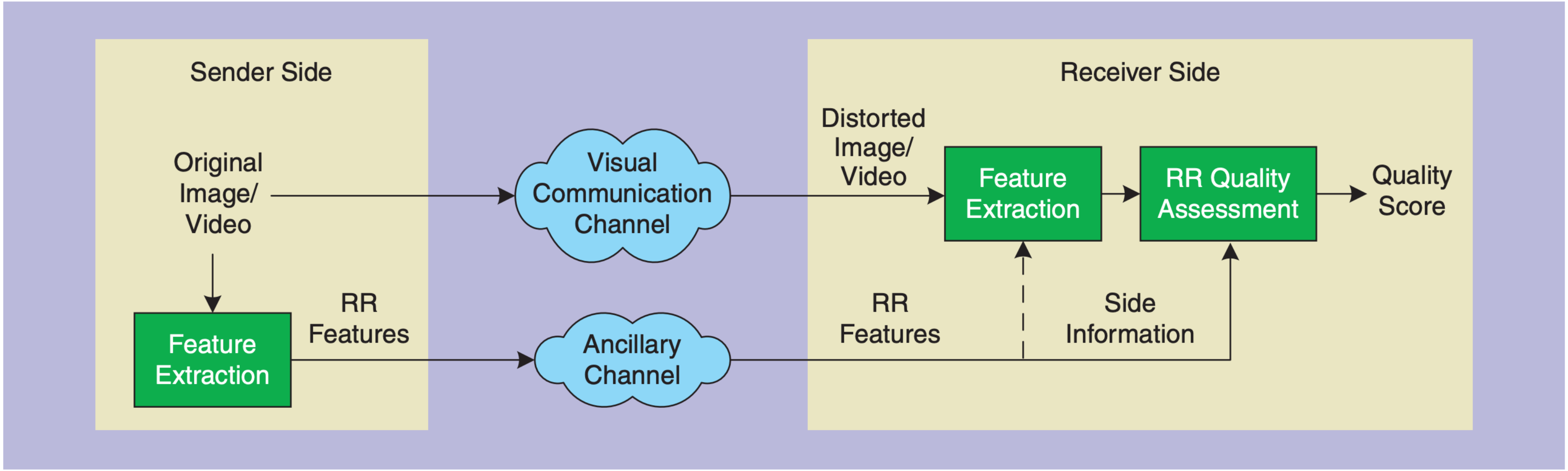

[FIG2] **General framework of an RR image or image QA system.**

Credit: Wang *et al.*, Reduced- and No-Reference Image Quality Assessment, In IEEE Signal Processing Magazine'11

Current Related Work of No-Reference / Blind IQA

- **Distortion-Specific Modeling**

  aware the image distortion types → build distortion-specific models

- **General NR-IQA Modeling**

  (1) Natural Scene Statistics Modeling

  Spatial Domain and Transform Domain

  (2) Human Visual System Modeling

  CNN modeling methods, assisted with visual importance information, reference images‘ information during training, ranking-based methods, graph representation learning, etc.

  (3) Codebook-based Modeling

  constructing a codebook

Selected Recent Progress on No-reference IQA

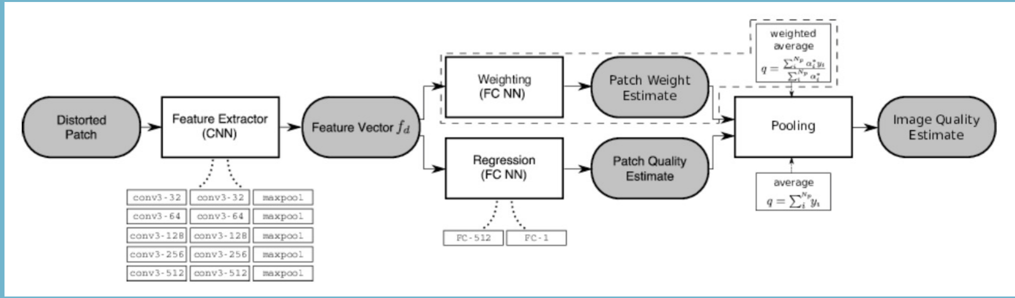

CNN-based Methods [1]

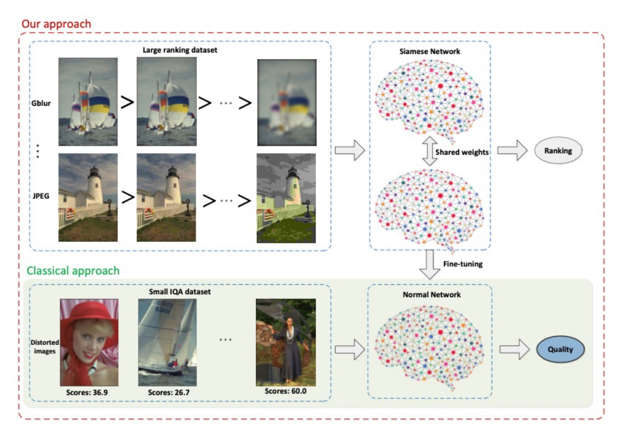

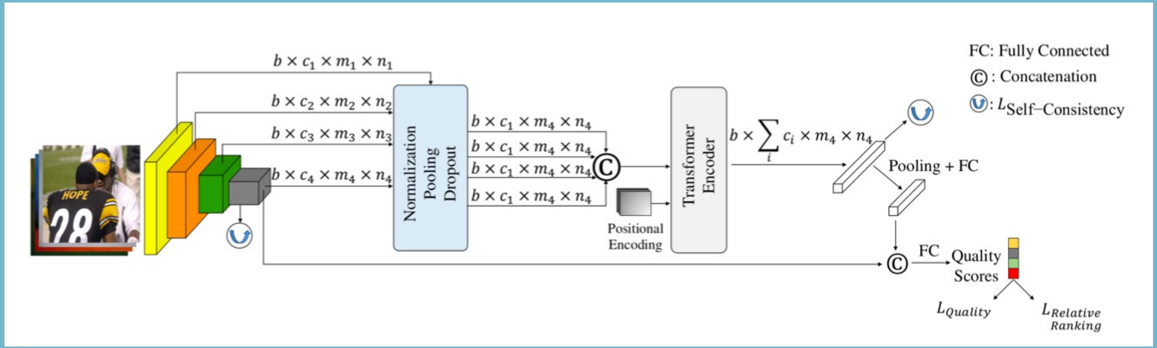

Ranking-based Methods [2]

Transformer-based Methods [3]

Credit:
[1] Bosse *et al.*, Deep Neural Networks for No-Reference and Full-Reference Image Quality Assessment, In IEEE TIP'18
[2] Liu *et al.*, RankIQA: Learning from Rankings for No-reference Image Quality Assessment, In ICCV'17
[3] Golestaneh *et al.*, No-Reference Image Quality Assessment via Transformers, Relative Ranking, and Self-Consistency, In WACV'22

Challenges

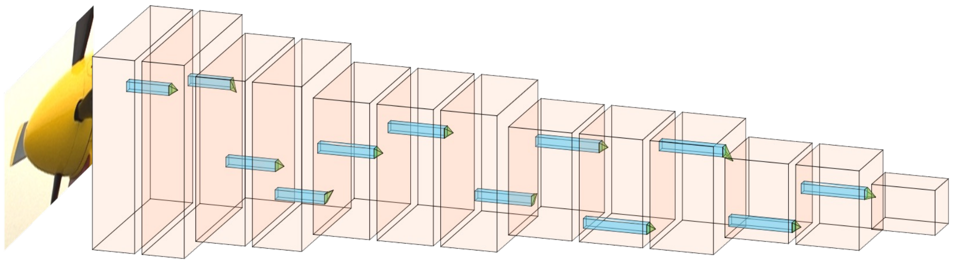

- Local Modeling (Convolutional Neural Networks):
  - ✓ Translation Invariance (Pooling)
  - ✓ Translation Equivalence (Convolution)
  - ✓ Sharable Fewer Parameters (Weight Sharing)
- Limitations:
  - ✓ Small-sized Receptive Field → **Extracted features are too local**
  - ✓ Parameters Fixed across the whole image → **Image content is equally treated**
  - ✓ Lack of Geometric and Relational Modeling → **Missing complex relations and dependencies**

Motivation

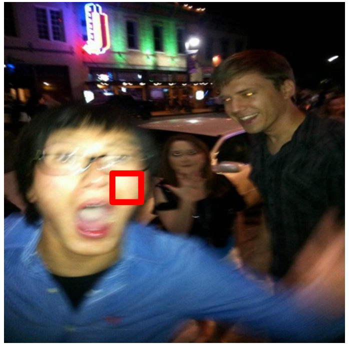

Local Feature Extraction

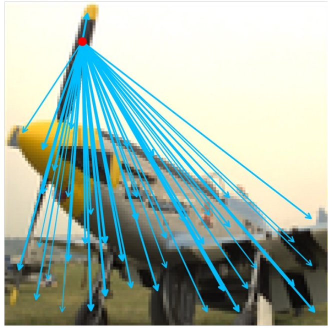

Non-local Dependency

✓ HVS is <u>**adaptive to the local content**</u>

→ ***Local feature extraction*** via a pre-trained CNN

✓ HVS perceives image quality with <u>**long-range dependency constructed among different regions**</u>

→ ***Non-local feature extraction*** for long-range dependency and relational modeling

Image Credit: LIVEC and TID2013 Databases

Definition

Non-Local:
Object-to-Pixel Modeling

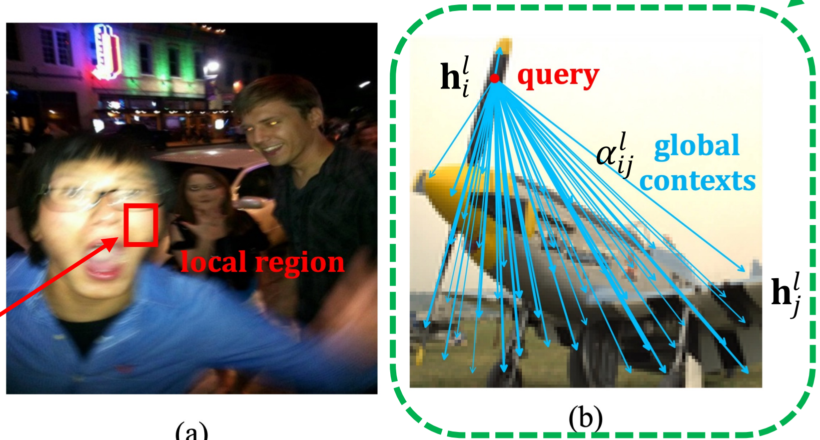

Convolution:
Pixel-to-Pixel Modeling

(a)
Local feature extraction is critical

(b)
Non-local dependency learned by the NLNet

Figure 2: Local region feature extraction and non-local dependency feature extraction

Spatial Integration of Information

$$\mathbf{h}_i^l = \mathrm{ELU}\left(\sum_{j \in \mathcal{N}(i)} \alpha_{ij}^l \mathbf{W}^l \mathbf{h}_j^l\right)$$

Spatial Weighting Functions

$$\alpha_{ij}^l = \frac{\exp(\mathrm{a}_{ij}^l)}{\sum_{k \in \mathcal{N}(i)} \mathrm{a}_{ik}^l}$$

$$\mathrm{a}_{ij}^l = \mathrm{LeakyReLU}(\mathrm{FC}([\mathbf{W}^l \mathbf{h}_i^l \parallel \mathbf{W}^l \mathbf{h}_j^l]))$$

- ✓ **Local Modeling**: encodes spatially proximate **Local Neighborhoods**.
- ✓ **Non-local Modeling**: establishes **Spatial Integration of Information** by **Long- and Short-Range Communications** with **different Spatial Weighting Functions**.

Image Credit: TID2013 and LIVEC Databases

Non-local Behavior

Object-to-Pixel Modeling
Region Feature Extraction

Non-local Dependency & Relational Modeling

Semantics and Content Understanding

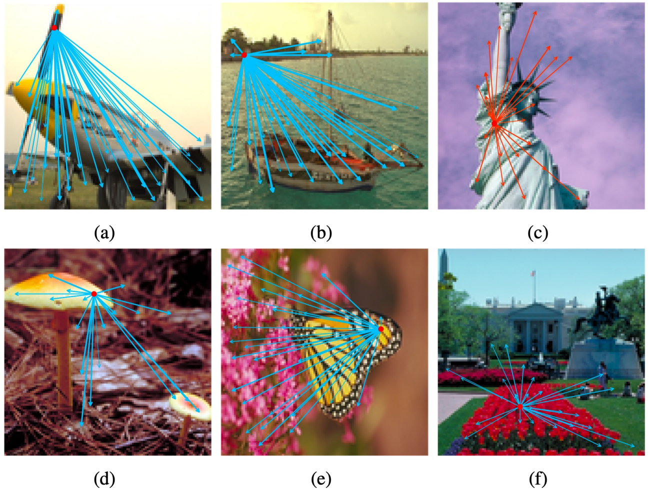

Figure 3.1: The non-local behavior of the long-range dependency and relational modeling. (a) The plane image with a query on wings. (b) The boat image with a query on nearby river bank. (c) The Statue of Liberty image with a query on the lady. (d) The shrooms image with a query on one shroom. (e) The butterfly image with a query on the wing. (f) The Lafayette Square, Washington, D.C. image with a query on flowers.

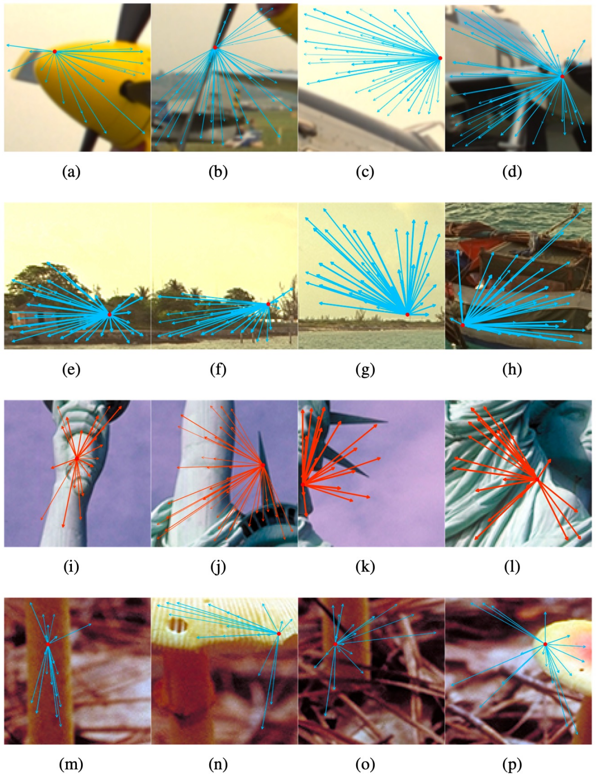

Figure 3.2: Selected demonstrations of the non-local behavior and long-range dependencies with regard to the cropped image patches from the illustrated images. The details of Figure (a) to (p) are described in the thesis.

✓ **Non-local Modeling**: establishes the **Spatial Integration of Information** by **Long- and Short-Range Communications** with **different Spatial Weighting Functions**.

Image Credit: TID2013 and LIVE Databases

Definition

Local Distortion

Non-Local Recurrence

Figure 4.9: Demonstrations of the global distortions (b/f: GB, c/g: CC, d/h: PN) contaminating the Statue of Liberty and George Rogers Clark Memorial images. Figure (a) and Figure (e) are reference images from the CSIQ database.

Global Distortion

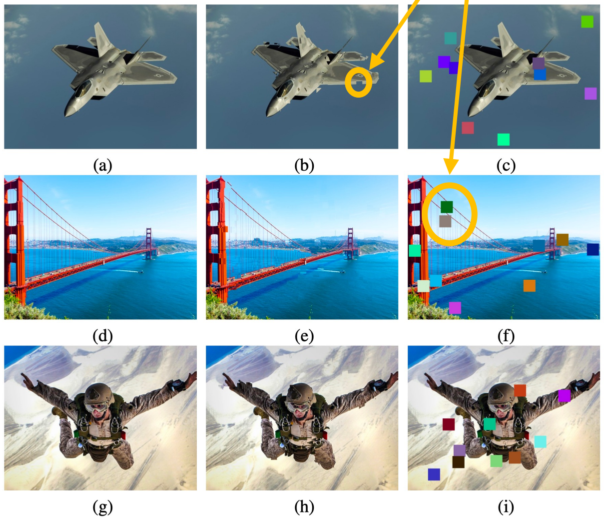

Figure 4.11: Demonstrations of the local distortions (b/e/h: non-eccentricity patch and c/f/i: color block). Figure (a), Figure (d), and Figure (g) are reference images from the KADID-10k database.

Local Distortion

Global Distortion: **globally and uniformly distributed** distortions with **non-local recurrences** over the image.

Local Distortion: **local nonuniform-distributed** distortions **in a local region**.

Image Credit: CSIQ and KADID-10k Databases

Superpixel Segmentation

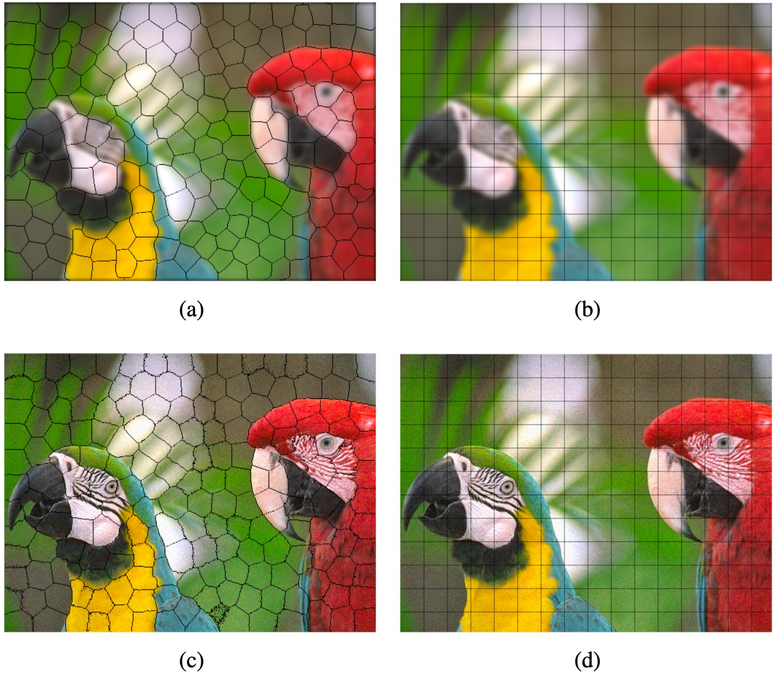

Figure 4.2: The superpixel *vs.* square patch representation (with size of $\approx 32 \times 32$) of the plane image from the TID2013 database.

Superpixel *vs.* Square Patch

- ✓ Adherence to boundaries and visually meaningful
- ✓ Accurate feature extraction

Image Credit: TID2013 Database

Superpixel Segmentation

Reference

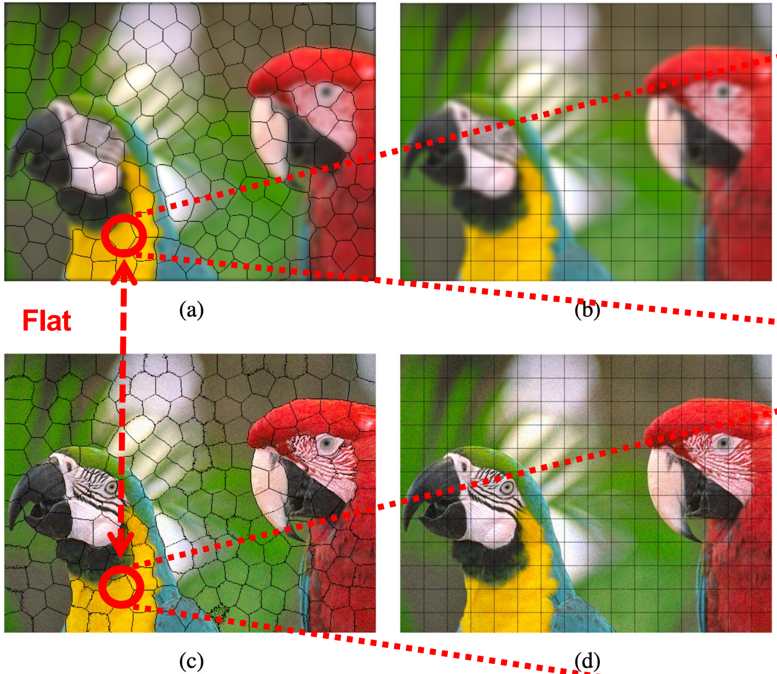

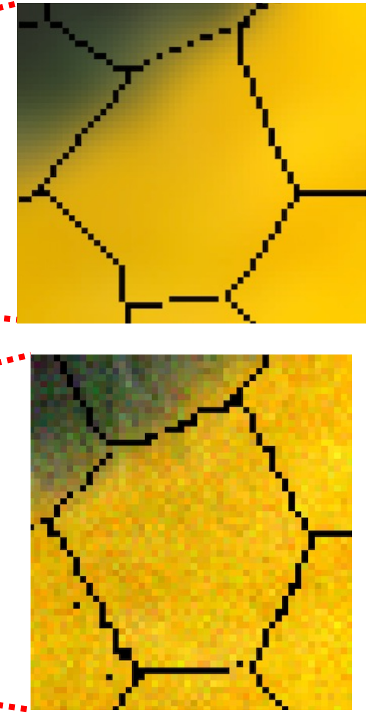

Gaussian Blur

Gaussian Noise

Figure 4.2: The superpixel *vs.* square patch representation (with size of $\approx 32 \times 32$) of the plane image from the TID2013 database.

Image Credit: TID2013 Database

Superpixel Segmentation

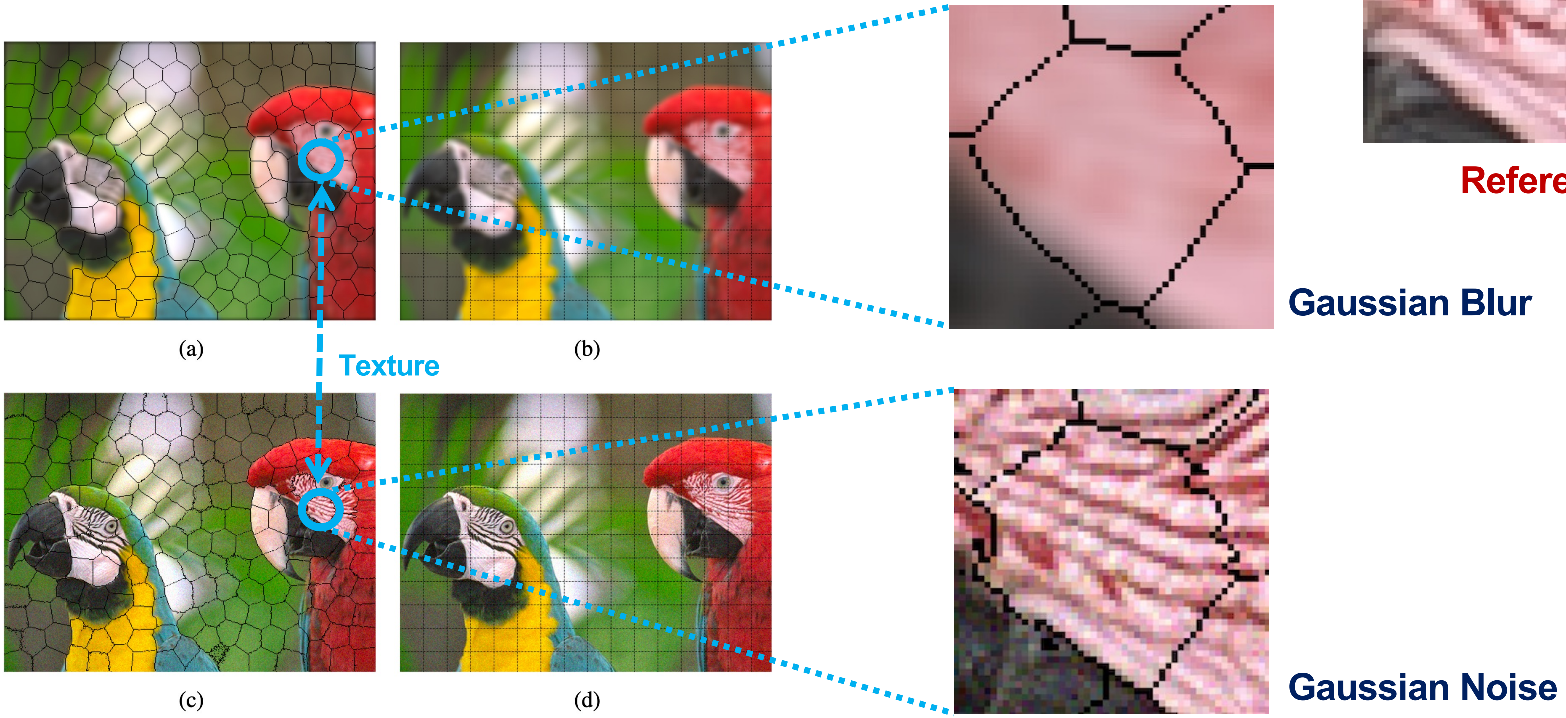

Figure 4.2: The superpixel *vs.* square patch representation (with size of $\approx 32 \times 32$) of the plane image from the TID2013 database.

Image Credit: TID2013 Database

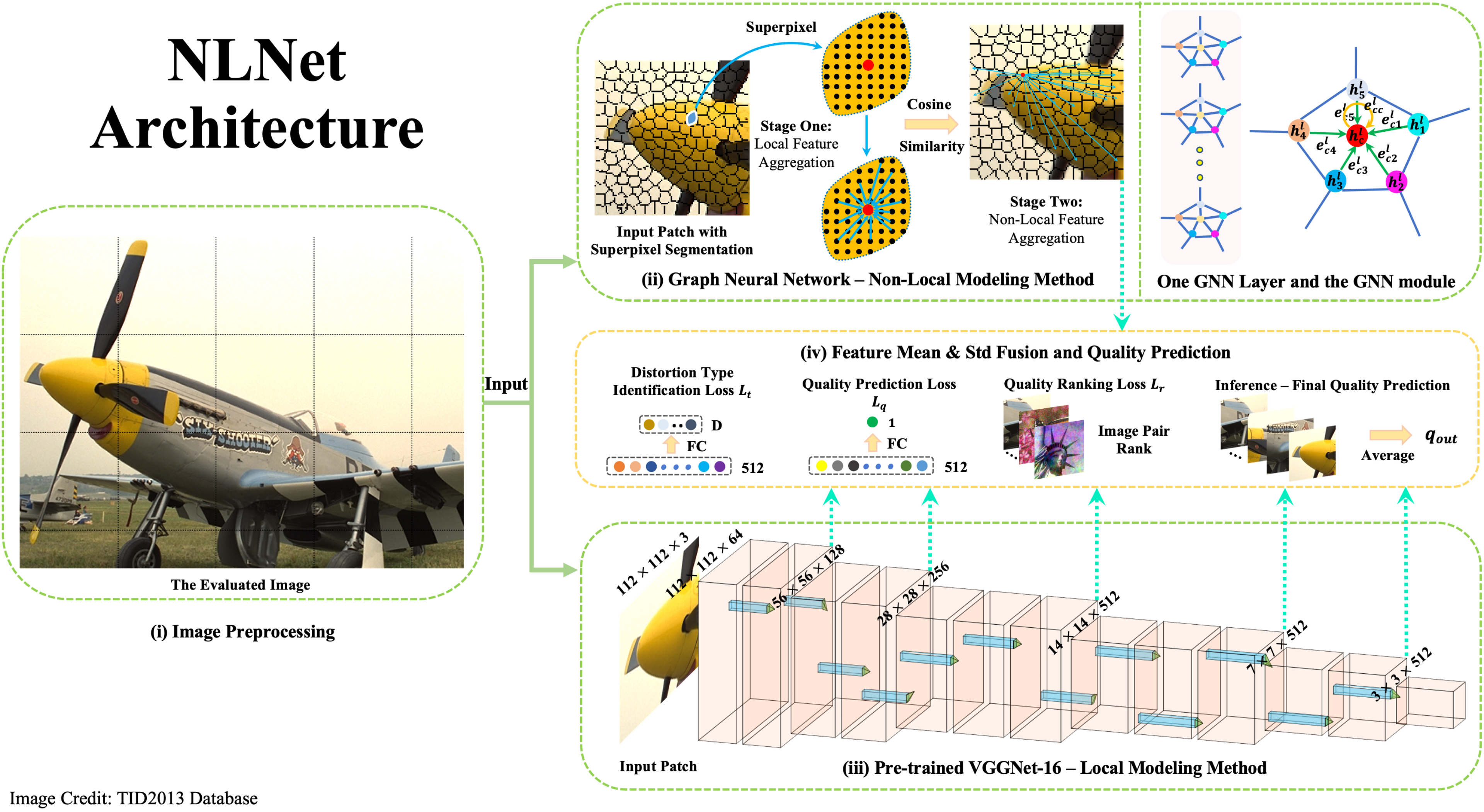
NLNet
Architecture
The Evaluated Image
(i) Image Preprocessing
Input
Superpixel
Input Patch with
Superpixel Segmentation
Stage One:
Local Feature
Aggregation
Cosine
Similarity
Stage Two:
Non-Local Feature
Aggregation
(ii) Graph Neural Network – Non-Local Modeling Method
One GNN Layer and the GNN module
(iv) Feature Mean & Std Fusion and Quality Prediction
Distortion Type
Identification Loss L_t
D
FC
512
Quality Prediction Loss
L_q
1
FC
512
Quality Ranking Loss L_r
Image Pair
Rank
Inference – Final Quality Prediction
Average
q_{out}
112 × 112 × 3
112 × 112 × 64
56 × 56 × 128
28 × 28 × 256
14 × 14 × 512
7 × 7 × 512
3 × 3 × 512
Input Patch
(iii) Pre-trained VGGNet-16 – Local Modeling Method
Image Credit: TID2013 Database

Experimental Setup

Databases:

✓ LIVE, CSIQ, TID2013, and KADID-10k

Experimental Settings:

✓ Intra-Database Experiments:

→ 60% training, 20% validation, and 20% testing, with `random` seeds from 1 to 10

→ The median SRCC and PLCC are reported.

✓ Cross-Database Evaluations:

→ One database as the training set, and the other databases as the testing set

→ Report the last epoch's performance

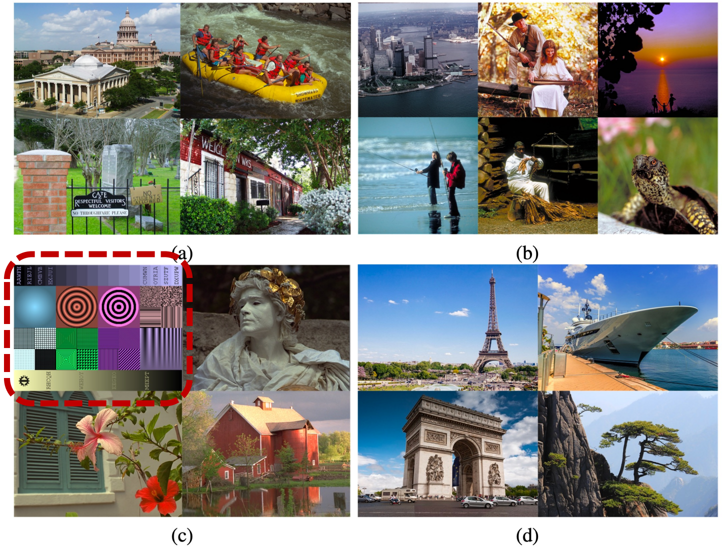

Figure 1.1: Natural images and a screen content image from the constructed databases. (a) LIVE Database [13] (b) CSIQ Database [14] (c) TID2013 Database [15] (d) KADID-10k Database [16].

Table 4.1: Brief summary of the LIVE, CSIQ, TID2013, and KADID-10k databases.

Database	LIVE [13]	CSIQ [14]	TID2013 [15]	KADID-10k [16]
Num. of Reference Images	29	30	25	81
Num. of Distorted Images	779	866	3,000	10,125
Num. of Distortion Types	5	6	24	25
Num. of Distortion Levels	$5 \sim 8$	$3 \sim 5$	5	5
Annotation	DMOS	DMOS	MOS	MOS
Range	[0, 100]	[0, 1]	[0, 9]	[1, 5]

Intra-Database Experiments

Table 4.2: Performance comparisons on the LIVE, CSIQ, and TID2013 databases. Top two results are highlighted in bold.

Method	LIVE		CSIQ		TID2013	
	SRCC	PLCC	SRCC	PLCC	SRCC	PLCC
BRISQUE (2012) [10]	0.939	0.935	0.746	0.829	0.604	0.694
CORNIA (2012) [104]	0.947	0.950	0.678	0.776	0.678	0.768
M3 (2015) [105]	0.951	0.950	0.795	0.839	0.689	0.771
HOSA (2016) [103]	0.946	0.947	0.741	0.823	0.735	0.815
FRIQUEE (2017) [90]	0.940	0.944	0.835	0.874	0.68	0.753
DIQaM-NR (2018) [35]	0.960	**0.972**	-	-	0.835	0.855
DB-CNN (2020) [64]	0.968	**0.971**	**0.946**	**0.959**	0.816	0.865
HyperIQA (2020) [65]	0.962	0.966	0.923	0.942	0.729	0.775
GraphIQA (2022) [86]	**0.968**	0.970	0.920	0.938	-	-
TReS (2022) [87]	**0.969**	0.968	0.922	0.942	**0.863**	**0.883**
NLNet	0.962	0.963	**0.941**	**0.958**	**0.856**	**0.880**

SOTA Transformer

Fewer Training Data
↓ 20% Total Data
↑ Highly Competitive Performance

Table 4.3: Performance comparisons on the KADID-10k database. Top two results are highlighted in bold.

Method	BRISQUE [10]	CORNIA [104]	HOSA [103]	InceptionResNetV2 [16]	DB-CNN [64]	HyperIQA [65]	TReS [87]	**NLNet**
SRCC	0.519	0.519	0.609	0.731	0.851	**0.852**	**0.859**	0.846
PLCC	0.554	0.554	0.653	0.734	**0.856**	0.845	**0.858**	0.850

Cross-Database Settings and Evaluations

Table 4.9: Cross-database performance comparisons.

Training	LIVE		CSIQ		TID2013	
Testing	CSIQ	TID2013	LIVE	TID2013	LIVE	CSIQ
BRISQUE (2012) [10]	0.562	0.358	0.847	0.454	0.790	0.590
CORNIA (2012) [104]	0.649	0.360	0.853	0.312	0.846	0.672
M3 (2015) [105]	0.621	0.344	0.797	0.328	0.873	0.605
HOSA (2016) [103]	0.594	0.361	0.773	0.329	0.846	0.612
FRIQUEE (2017) [90]	0.722	0.461	0.879	0.463	0.755	0.635
DIQaM-NR (2018) [35]	0.681	0.392	-	-	-	0.717
DB-CNN (2020) [64]	**0.758**	**0.524**	0.877	**0.540**	**0.891**	**0.807**
HyperIQA (2020) [65]	0.697	**0.538**	**0.905**	**0.554**	0.839	0.543
NLNet	**0.771**	0.497	**0.923**	0.516	**0.895**	**0.730**

Similar Distortions

TID: More Distortion Types & Levels

Single Distortion Type Evaluation

Table 4.4: The average SRCC and PLCC results of the individual distortion type on the LIVE database. Top two results are highlighted in bold.

SRCC	Global Distortion				Local Distortion
	JPEG	JP2K	WN	GB	FF
BRISQUE (2012) [10]	0.965	0.929	0.982	**0.964**	0.828
CORNIA (2012) [104]	0.947	0.924	0.958	0.951	0.921
M3 (2014) [105]	0.966	0.930	**0.986**	0.935	0.902
HOSA (2016) [103]	0.954	0.935	0.975	0.954	**0.954**
FRIQUEE (2017) [90]	0.947	0.919	0.983	0.937	0.884
dipIQ (2017) [82]	0.969	**0.956**	0.975	0.940	-
WaDIQaM (2018) [35]	0.953	0.942	0.982	0.938	0.923
DB-CNN (2020) [64]	**0.972**	0.955	0.980	0.935	0.930
HyperIQA (2020) [65]	0.961	0.949	0.982	0.926	0.934
NLNet	**0.979**	**0.958**	**0.990**	**0.964**	**0.941**
PLCC	Global Distortion				Local Distortion
	JPEG	JP2K	WN	GB	FF
BRISQUE (2012) [10]	0.971	0.940	0.989	**0.965**	0.894
CORNIA (2012) [104]	0.962	0.944	0.974	0.961	0.943
M3 (2014) [105]	0.977	0.945	**0.992**	0.947	0.920
HOSA (2016) [103]	0.967	0.949	0.983	**0.967**	**0.967**
FRIQUEE (2017) [90]	0.955	0.935	0.991	0.949	0.936
dipIQ (2017) [82]	0.980	**0.964**	0.983	0.948	-
DB-CNN (2020) [64]	**0.986**	**0.967**	0.988	0.956	**0.961**
NLNet	**0.986**	0.961	**0.993**	0.964	0.951

Noisy and Compressed Images

Global Distortion

Non-local Recurrence

Local Distortion

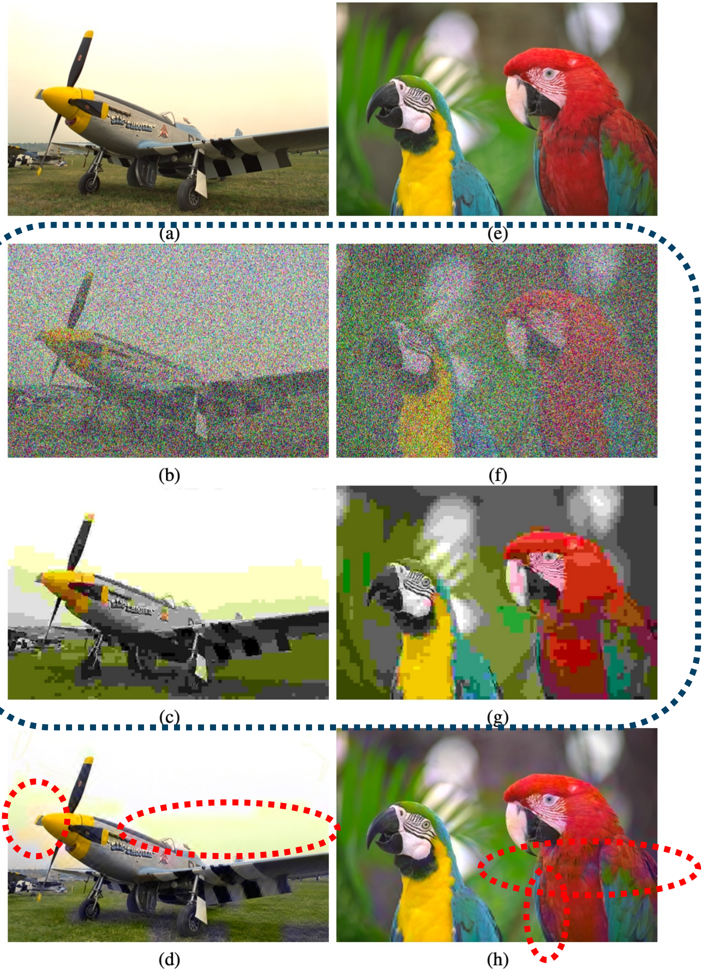

Figure 4.7: Demonstrations of the global distortions (b/f: WN and c/g: JPEG) and local distortions (d/h: FF) contaminating the plane and parrot images. Figure (a) and Figure (e) are reference images from the LIVE database.

Image Credit: LIVE Database

Single Distortion Type Evaluation

Table 4.5: The average SRCC and PLCC results of the individual distortion type on the CSIQ database. Top two results are highlighted in bold.

SRCC	JPEG	JP2K	WN	GB	PN	CC
BRISQUE (2012) [10]	0.806	0.840	0.723	0.820	0.378	0.804
CORNIA (2012) [104]	0.513	0.831	0.664	0.836	0.493	0.462
M3 (2014) [105]	0.740	0.911	0.741	0.868	0.663	0.770
HOSA (2016) [103]	0.733	0.818	0.604	0.841	0.500	0.716
FRIQUEE (2017) [90]	0.869	0.846	0.748	0.870	0.753	0.838
dipIQ (2017) [82]	0.936	0.944	0.904	0.932	-	-
MEON (2018) [71]	**0.948**	0.898	**0.951**	0.918	-	-
WaDIQaM (2018) [35]	0.853	0.947	0.974	0.979	0.882	**0.923**
DB-CNN (2020) [64]	0.940	0.953	0.948	**0.947**	**0.940**	0.870
HyperIQA (2020) [65]	0.934	**0.960**	0.927	0.915	0.931	0.874
NLNet	**0.972**	**0.963**	**0.965**	**0.955**	**0.969**	**0.968**
PLCC	JPEG	JP2K	WN	GB	PN	CC
BRISQUE (2012) [10]	0.828	0.887	0.742	0.891	0.496	0.835
CORNIA (2012) [104]	0.563	0.883	0.687	0.904	0.632	0.543
M3 (2014) [105]	0.768	0.928	0.728	0.917	0.717	0.787
HOSA (2016) [103]	0.759	0.899	0.656	0.912	0.601	0.744
FRIQUEE (2017) [90]	0.885	0.883	0.778	0.905	0.769	0.864
dipIQ (2017) [82]	0.975	**0.959**	0.927	0.958	-	-
MEON (2018) [71]	0.979	0.925	**0.958**	0.946	-	-
DB-CNN (2020) [64]	**0.982**	0.971	0.956	**0.969**	**0.950**	**0.895**
NLNet	**0.991**	**0.976**	**0.967**	**0.9746**	**0.966**	**0.969**

Noise-Related Distortions

Global Distortion

Figure 4.9: Demonstrations of the global distortions (b/f: GB, c/g: CC, d/h: PN) contaminating the Statue of Liberty and George Rogers Clark Memorial images. Figure (a) and Figure (e) are reference images from the CSIQ database.

Image Credit: CSIQ Database

Single Distortion Type Evaluation

Table 4.6: The average SRCC results of the individual distortion type on the TID2013 database. Top two results are highlighted in bold.

SRCC	Distortion Type	BRISQUE [10]	FRIQUEE [90]	HOSA [103]	MEON [71]	M3 [105]	DB-CNN [64]	CORNIA [104]	**NLNet**
Global Distortion	Additive Gaussian noise	0.711	0.730	**0.833** ↑8.4%	0.813	0.766	0.790	0.692	**0.917**
	Lossy compression of noisy images	0.609	0.641	0.838	0.772	0.692	**0.860** ↑7.5%	0.712	**0.935**
	Additive noise in color components	0.432	0.573	0.551	**0.722** ↑12.8%	0.5[illegible]0	0.700	0.137	**0.850**
	Comfort noise	0.196	0.318	0.622	0.406	0.353	**0.752** ↑11.8%	0.617	**0.870**
	Contrast change	-0.001	**0.585**	0.362	0.252	0.155	0.548	0.254	**0.793**
	Change of color saturation	0.003	0.589	0.045	**0.684**	-0.199	0.631	0.169	**0.827**
	Spatially correlated noise	0.746	0.866	0.842	**0.926** ↑3.2%	0.782	0.826	0.741	**0.958**
	High frequency noise	0.842	0.847	0.897	**0.911** ↑1.0%	0.900	0.879	0.815	**0.921**
	Impulse noise	0.765	0.730	0.809	**0.901** ↑1.2%	0.738	0.708	0.616	**0.913**
	Quantization noise	0.662	0.764	0.815	**0.888** ↑4.1%	0.832	0.825	0.661	**0.929**
	Gaussian blur	0.871	0.881	0.883	0.887	**0.896**	0.859	0.850	**0.912**
	Image denoising	0.612	0.839	0.854	0.797	0.709	**0.865** ↑1.7%	0.764	**0.882**
	JPEG compression	0.764	0.813	0.891	0.850	0.844	**0.894** ↑1.1%	0.797	**0.905**
	JPEG 2000 compression	0.745	0.831	**0.919** ↑1.1%	0.891	0.885	0.916	0.846	**0.930**
	Multiplicative Gaussian noise	0.717	0.704	0.768	**0.849** ↑5.5%	0.738	0.711	0.593	**0.904**
	Image color quantization with dither	0.831	0.768	0.896	0.857	**0.908**	0.833	0.683	**0.911**
	Sparse sampling and reconstruction	0.807	0.891	**0.909**	0.855	0.893	0.902	0.865	**0.940**
	Chromatic aberrations	0.615	0.737	0.753	**0.779**	0.570	0.732	0.696	**0.773**
	Masked noise	0.252	0.345	0.468	**0.728**	0.577	0.646	0.451	**0.700**
	Mean shift (intensity shift)	0.219	**0.254**	0.211	0.177	0.119	-0.009	0.232	**0.358**
Local Distortion	JPEG transmission errors	0.301	0.498	0.730	0.746	0.375	**0.772** ↑3.3%	0.694	**0.805**
	JPEG 2000 transmission errors	0.748	0.660	0.710	0.716	0.718	**0.773** ↑10.2%	0.686	**0.875**
	Non eccentricity pattern noise	0.269	0.076	0.242	0.116	0.173	**0.270** ↑34.6%	0.200	**0.616**
	Local bock-wise distortions with different intensity	0.207	0.032	0.268	**0.500**	0.379	0.444	0.027	**0.493**

Noise and Compression-Related Distortions

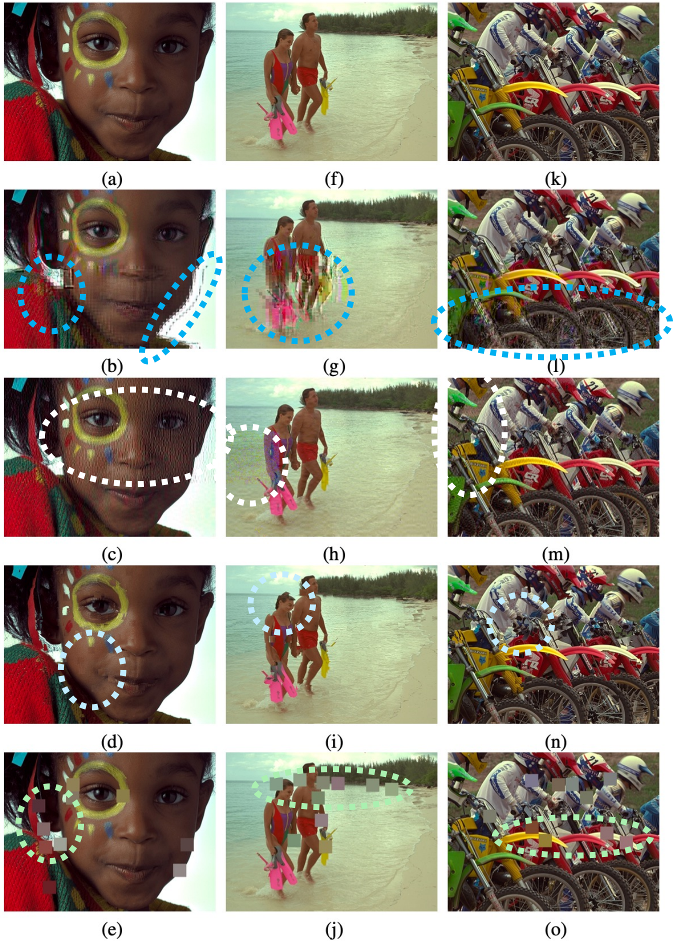

Figure 4.10: Demonstrations of the local distortions (b/g/l: JPEG transmission errors, c/h/m: JPEG2000 transmission errors, d/i/n: non eccentricity pattern noise, e/j/o: local block-wise distortions of different intensity). Figure (a), Figure (f), and Figure (k) are reference images from the TID2013 database.

Image Credit: TID2013 Database

Single Distortion Type Evaluation

Table 4.7: The average SRCC results of the individual distortion type on the KADID-10k database. The local distortions are highlighted in blue and the top two results are highlighted in bold.

Distortion Type		BLIINDS-II [91]	BRISQUE [10]	ILNIQE [102]	CORNIA [104]	HOSA [103]	WaDIQaM [35]	**NLNet**
Blurs	Lens blur	0.781	0.674	**0.846**	0.811	0.715	0.730	**0.914**
	Gaussian blur	0.880	0.812	**0.883**	0.866	0.852	0.879	**0.914**
	Motion blur	0.482	0.423	**0.779**	0.532	0.652	0.730	**0.899**
Color distortions	Color diffusion	0.572	0.544	0.678	0.243	0.727	**0.833**	**0.916**
	Color saturation 2	0.602	0.375	0.677	0.120	**0.841**	0.836	**0.909**
	Color quantization	0.670	0.667	0.676	0.323	0.662	**0.806**	**0.853**
	Color shift	-0.139	-0.182	0.090	-0.002	0.050	**0.421**	**0.777**
	Color saturation 1	0.091	0.071	0.027	-0.019	**0.216**	0.148	**0.604**
Compression	JPEG compression	0.414	0.782	**0.804** ↑6.2%	0.556	0.582	0.530	**0.866**
	JPEG 2000 compression	0.655	0.516	**0.790** ↑6.3%	0.342	0.608	0.539	**0.853**
Noise	Denoise	0.457	0.221	**0.856** ↑9.7%	0.229	0.247	0.765	**0.953**
	White noise in color component	0.757	0.718	0.841	0.418	0.745 ↑1.1%	**0.925**	**0.936**
	Multiplicative noise	0.702	0.674	0.682	0.306	0.776 ↑5.0%	**0.884**	**0.934**
	Impulse noise	0.547	-0.543	0.808	0.219	0.254 ↑10.2%	**0.814**	**0.916**
	White Gaussian noise	0.628	0.708	0.776	0.357	0.680 ↑1.7%	**0.897**	**0.914**
Brightness change	Brighten	0.458	0.575	0.301	0.227	**0.753**	0.685	**0.822**
	Darken	0.439	0.405	0.436	0.206	**0.744**	0.272	**0.647**
	Mean Shift	0.112	0.144	0.315	0.122	**0.591**	**0.348**	0.335
Spatial distortions	Jitter	0.629	0.672	0.441	0.719	0.391	**0.778**	**0.899**
	Pixelate	0.196	0.648	0.577	0.587	**0.702**	0.700	**0.814**
	Quantization	**0.781**	0.714	0.571	0.259	0.681	0.735	**0.791**
	Color block	-0.020	0.067	0.003	0.094	**0.388**	0.160	**0.440**
	Non-eccentricity patch	0.083	0.191	0.218	0.121	**0.461**	0.348	**0.433**
Sharpness and contrast	High sharpen	-0.015	0.361	**0.681**	0.114	0.230	0.558	**0.932**
	Contrast change	0.062	0.105	0.072	0.125	**0.452**	0.421	**0.513**

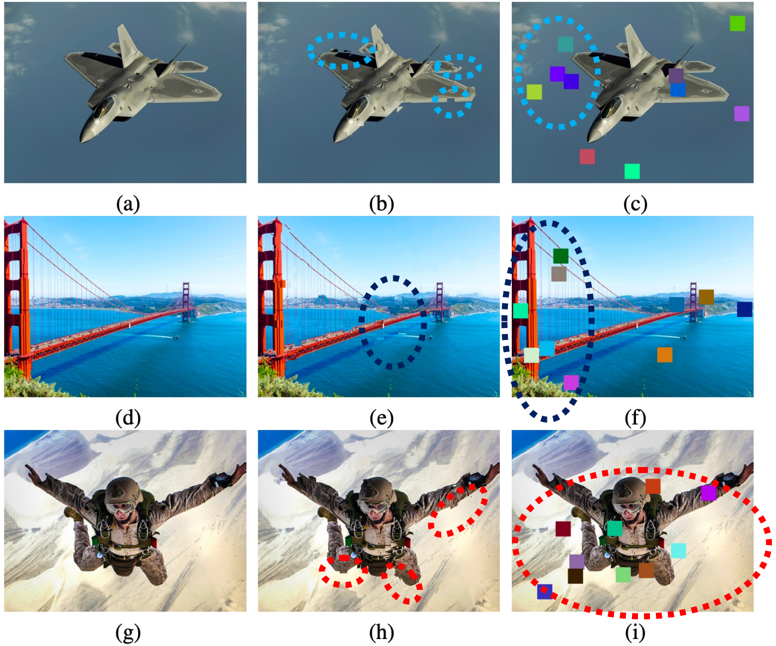

Figure 4.11: Demonstrations of the local distortions (b/e/h: non-eccentricity patch and c/f/i: color block). Figure (a), Figure (d), and Figure (g) are reference images from the KADID-10k database.

Image Credit: KADID-10k Database

Takeaways and Future Work

✓ Non-local & Local Modeling

(1) The Non-local Modeling is complementary to traditional local methods.

(2) CNN's Local Modeling features are effective and robust.

✓ Global & Local Distortions

(1) Handle a wide variety of Global Distortions: globally and uniformly distributed with non-local recurrences.

(2) Maintain sensitivity to Local Distortions: local nonuniform-distributed distortions in a local region.

(3) Better assess Noisy and Compressed Images quality.

✓ Generalization Capability Cross-Dataset Setting → High Generalization Capability

✓ Future Work Non-local Statistics [1, 2]; PGC → UGC → AIGC: Quality Assessment of AI Generated Content

Credit:
[1] Zontak *et al.*, Internal Statistics of a Single Natural Image, In CVPR 2011
[2] Buades *et al.*, A Non-local Algorithm for Image Denoising, In CVPR 2005